Influence of gas media and low pressure on the dynamics of wetting transition of laser textured stainless steel meshes during air ageing

Vyacheslav V. Kim[1], Sharjeel Ahmed Khan[1], Vadim Sh. Yalishev[1], Mazhar Iqbal[1], Ganjaboy S. Boltaev[1], Rashid A. Ganeev[1], and Ali S. Alsaner[1]

[1]American University of Sharjah

October 1, 2020

Abstract

We analyze the role of the processing atmosphere and influence of long term ageing (up to 30 days) in ambient air on the wettability of the laser-processed stainless steel meshes. The effect of low-pressure and vacuum ageing transform the initial superhydrophilic characteristics of freshly laser structured mesh to near superhydrophobic state. Laser texturing of meshes was carried out in the presence of different gas environmental conditions: N 2 , O 2 , CO 2 , Ar, SF 6 , ambient atmospheric air and under different vacuum conditions. The influence of each gas on the time evolution of the wettability properties after ageing in ambient air is analyzed.

Influence of gas media and low pressure on the dynamics of wetting transition of laser textured stainless steel meshes during air ageing

Vyacheslav V. Kim[1], Sharjeel A. Khan[1], Vadim Sh. Yalishev[1], Mazhar Iqbal[1],

Ganjaboy S. Boltaev[1], Rashid A. Ganeev[1], and Ali S. Alnaser[1*]

[1] *Department of Physics, American University of Sharjah, Sharjah 26666, UAE*

[*] *Corresponding author:*{aalnaser@aus.edu}

Abstract: We analyze the role of the processing atmosphere and influence of long term ageing (up to 30 days) in ambient air on the wettability of the laser-processed stainless steel meshes. The effect of low-pressure and vacuum ageing transform the initial superhydrophilic characteristics of freshly laser structured mesh to near superhydrophobic state. Laser texturing of meshes was carried out in the presence of different gas environmental conditions: N_2, O_2, CO_2, Ar, SF_6, ambient atmospheric air and under different vacuum conditions. The influence of each gas on the time evolution of the wettability properties after ageing in ambient air is analyzed.

KEYWORDS

Stainless steel mesh, superhydrophobic, superhydrophilic, vacuum ageing, air ageing

Introduction

The wettability of a material's surface is an important property that plays a crucial role in the wide range of surface-related phenomena's and defines different ranges of applications where materials can be used. In the case of stainless steel, the industrial applications are countless and can be enhanced by controlling its surface properties. Surface properties of steel such as color, chemical stability, roughness, and wettability

have received special attention in biomedicine, optics and surface chemistry [1-4]. Stainless steel in form of meshes is a robust, durable and flexible construction material. Recently, controlling the wettability state of the metal meshes by femtosecond laser-induced structuring has found applications for efficient oil-water separation [5,6]. Wetting is the ability of a liquid medium to maintain contact with a solid medium due to intermolecular interaction when in contact with each other. Static contact angle ϑ is a quantitative way to measure wettability at a solid-liquid interface [7]. In our work the liquid is water and is termed as static water contact angle ϑ_{w}. Different strategies have been proposed to tune the wetting behavior of metal surfaces. Most of them require the use of coatings using suitable materials or plasma/chemical etching. Recently, controlling the extreme wetting properties of materials by laser texturing of the substrate has gained much attention because it is maskless, chemical free, facile and robust technique [8].

Laser texturing of metal surfaces is proven to be a reliable way to change wettability of materials, with transitions towards the superhydrophilic or superhydrophobic properties depending on the material surface energy. For low surface energy material like polytetrafluoroethylene (Teflon) laser structuring can enhance the superhydrophobic characteristic [9]. Whereas, for other freshly laser textured materials it yields superhydrophilic response [10,11]. Laser processing of metals in ambient air by femtosecond laser pulses produces metal oxides on the textured surfaces. Metal oxides possess high surface energy and typically behave as hydrophilic material because oxides favour formation of hydroxylated layer through hydrogen bonding [12]. Laser texturing leads to formation of various micro- and nanostructures on the surface of the material. Shape and content of these structures can be controlled by laser parameters, such as pulse energy, polarization, scanning strategy and so on. Generally, laser surface structuring is accompanied with functionalization step to alter or retain the desirable surface wettability of materials. Typically, extreme wettability of laser textured surfaces was achieved through toxic and complex chemical reagent causing harm to the environment.

Moreover, the wettability of laser-textured metal surfaces can be changed from hydrophilic to hydrophobic if the textured surface is exposed to air for an extended period of time. Such transitions were observed for stainless steel [11,13], aluminum alloys [10, 14] and other metal alloys [15,16]. This transition is also observed for micro/nanostructures textured using the pulsed lasers operating in the nanosecond, picosecond and femtosecond time domains.

Generally, surfaces after the laser treatment are hydrophilic ($\vartheta_{\mathrm{w}} < 30^{\circ}$). Within one week of exposure in air, the wettability changes to hydrophobic (ϑ_{w} [?] 90°), and within two weeks or more the surfaces become superhydrophobic with ϑ_{w} [?] 150°. The exposure to air does not change the morphology of the micro/nanostructures. However, the surface is influenced by chemical changes. Different processing environments including O_2, air, N_2, CO_2, and Ar during laser texturing of AISI 304 stainless steel were studied in [17]. In one study, the textured samples were kept in sterile individual plastic bags filled with air for 7 days. It was shown that after 7 days the surface textured in argon environment achieves $\vartheta_{\mathrm{w}} = 125^{\circ}$, whereas surfaces processed in oxygen, air, carbon dioxide, and nitrogen had $\vartheta_{\mathrm{w}} = 31^{\circ}$, 46°, 50°, and 83°, respectively. XPS study demonstrated a significant amount of carbon on the surface, indicating the adsorption of organic or biomolecules during storage in sterile individual plastic bags. Those studies have shown that laser processing ageing environment influences the wettability transition rate.

Analysis of laser textured aluminum was performed previously [10] to identify the mechanisms contributing to long term air exposure-induced wettability transition. After laser texturing in ambient air, aluminum oxide surfaces are known to have many polar sites composed of unsaturated aluminum and oxygen atoms, which lead to an overall hydrophilic surface [18]. The textured samples that were kept in N_2, O_2, and CO_2atmosphere remained superhydrophilic and these gases do not contribute to the wettability transition of aluminum. It was observed in [8] that surfaces kept in air and an atmosphere with volatile polar organics (4-Methyloctanoic acid) demonstrated a significant transition of wettability towards the superhydrophobicity. XPS analysis has shown that the amount of carbon on these surfaces and the carbon to aluminum ratio increased drastically over the same time periods. These measurements indicated that adsorbed organic compounds from ambient air are likely to form a hydrophobic coating on the initially hydrophilic metal-oxide surface.

In the present work, the role of the processing atmosphere, as well as the influence of the long term ageing in ambient air of the laser-processed stainless steel meshes on their wettability, are investigated. The role of low-pressure and vacuum ageing was also tested. Complex geometrical form and curved nature of meshes is crucial and not easy by itself and it was already demonstrated in [6]. In our work we focused on influence of processing atmosphere and subsequent long-term ageing on the wetting behaviour of laser treated meshes. For these purposes stainless steel mesh samples were processed in atmospheres of pure gases, ambient air and low pressure (vacuum) condition. After processing, long-term air ageing (30 days) was used to define the final wettability properties. We used 5 different gases - N_2, O_2, CO_2, Ar, SF_6, with the first three being part of the ambient air, which allows to define the possible role of these air components on the wetting properties after long-term air ageing. We also sufficiently decreased the role of water vapor during laser processing by conducting laser structuring inside closed chamber in pure gas atmospheres. Ar and vacuum conditions present inert conditions, whereas SF_6gas, which is not a component of ambient air, can potentially affects the etching and enriching of samples surfaces with fluorine and its compounds.

Experimental setup

Meshes were processed by laser radiation in the presence of five gases (N_2, O_2, CO_2, Ar, SF_6), as well as in ambient atmospheric air and in vacuum conditions. In contrast to [17] where the used gases were purged on the surface of the samples, which does not completely excludes the influence of ambient air. In our work the stainless steel meshes were laser processed in pure atmosphere of each individual gases introduced inside the vacuum pumped chamber. Also we are using the femtosecond laser source at 1030 nm wavelength while authors of [17] utilized the nanosecond source at $\lambda = 532$ nm. After processing, the laser-textured meshes were aged in the ambient air conditions for 30 days under the same conditions, while maintaining the constant temperature and humidity. To analyze the effect of vacuum ageing on the wetting characteristic, two different chambers were used. One of them utilized oil-free vacuum pump system, while second chamber used the pump containing oil as lubricant for the moving parts.

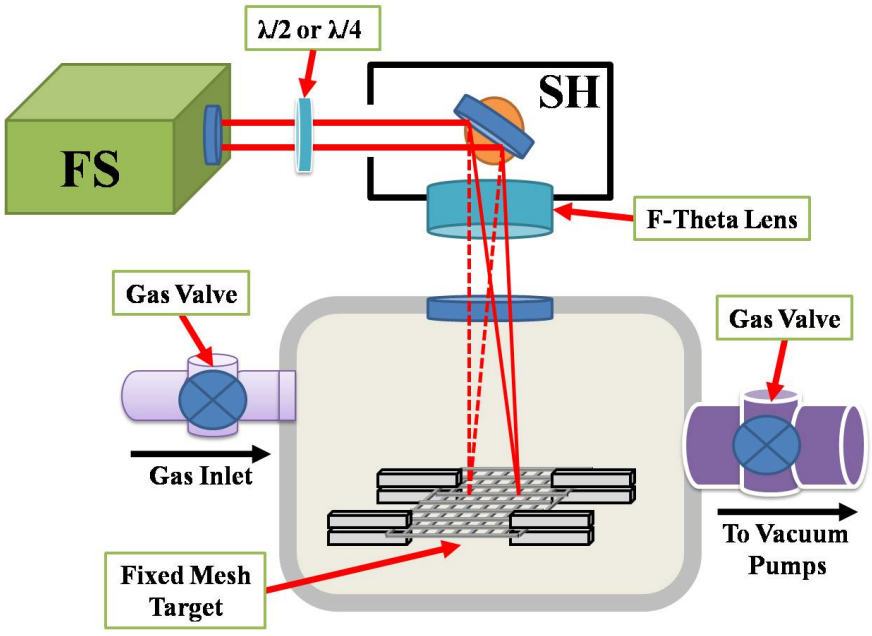

Figure 1. Experimental setup. Beam from femtosecond laser source (FS) was controlled by scanning head (SH) and focused inside the vacuum chamber on the surface of the mesh target. The polarization properties were controlled using $\lambda/2$ or $\lambda/4$ waveplates. Two gas valves were used to control gas pressure inside chamber or to keep vacuum conditions. Mesh target inside chamber was fixed in a way that no material existed behind

mesh pores and no deposition from any other material occurred.

Figure 1 shows the experimental setup used for laser treatment of the meshes in various gas atmospheres. 5 W laser beam (FS) from high-power fiber-based laser system (AFS-UFFL-300-2000-1030-300, Active Fiber Systems GmbH) with a central wavelength of 1030 nm, repetition rate of 50 kHz, and a pulse duration of 40 fs, was used for laser structuring of meshes. Laser radiation was focused and raster scanned on the sample by 160 mm F-Theta lens and scan head (SH) (FARO tech. Xtreme-20) as shown in Fig. 1. The scanning head was mounted outside the vacuum chamber and the scanning beam was directed inside the chamber through the quartz window. The laser surface texturing of the stainless meshes was carried out using similar geometry by bi-directional line-by-line scanning strategy. The distance between scan lines was set equal to 60 μm. The focused laser beam spot diameter was measured ~100 μm. Single laser pulse energy was equal to 100 μJ.

The samples of meshes with 2×2 cm size were textured inside the vacuum chamber in presence of different gases, atmospheric air or in the vacuum conditions. Gases (N_2, O_2, CO_2, Ar, SF_6) with 99.95% purity were used. The mesh inside chamber was fixed in a way that no material behind mesh pores gets existed and no deposition from any other material occurred. Scanning speed was varied from 50 to 300 mm/s. With the estimation of the focusing spot area it gives the laser fluence on the target area of 1.2 J/cm^2. The number of overlapped pulses was varied from 16 to 100. The polarization direction of laser beam was controlled by λ/2 waveplate. The circular polarization was obtained by using the λ/4 waveplate. Different vacuum pump systems were used in our experiments with two chambers, which we designate as Chamber #1 and Chamber #2. In Chamber #1, we used the pair of "oil-less" pumps (Edwards nXDS 6i and Pfeiffer HiPace 30 turbopump). Chamber #2 utilized another pair of pumps, one of which (Pfeiffer DUO 2.5) used the vacuum oil (Edwards Ultragrade 19) as a lubricant. In both chambers, the vacuum at 2×10^{-4} mbar was maintained during these experiments. Gas pressure was controlled by two gas valves. The first valve was placed before the vacuum pumps system, and the second one controlled the gas inlet.

Following laser treatment, the surface morphological analysis was performed using scanning electron microscope (SEM) (TESCAN VEGA3) and the surface chemistry was evaluated semi-quantitatively via energy-dispersive X-ray spectroscopy (EDS) technique using the SEM X-ray detector. For wettability characterization, water contact angle (WCA) was measured using Drop Shape Analyzer (KRUSS). Distilled water droplets (~5 μl volume) were used for all samples to determine WCA.

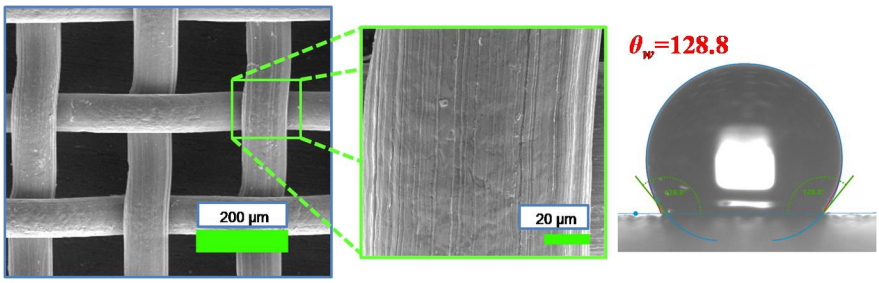

Figure 2. SEM images of the untreated stainless steel mesh and measured water contact angle.

Stainless steel meshes (316 L) with 150 μm pore size and 100 μm mesh wire thickness were used because of their high mechanical strength, durability and commercial availability. Meshes were purchased from Sigma-Aldrich. Figure 2 shows SEM images of the untreated mesh. Note that surface of wires had structures in the form of lines along wire direction and some irregularities at the positions of wires overlaps, which were resulted from the manufacturing method of wires and meshes. These structures with combination of meshes geometry could be responsible for the relatively high WCA for untreated meshes (~128°). After preparation, the laser textured meshes were aged in ambient air for 30 days under the same conditions, with supporting constant temperature and humidity (21.5° C and 45% humidity).

1. **Result and discussion**
2. Surface morphology

Firstly, we describe the process of samples preparation using different gases. Mesh samples were structured inside Chamber #1. The air at 1 atm was purged inside the chamber for laser treatment of meshes at ambient conditions. In the case of different gases the procedure was as follows. Initially we pumped the chamber with meshes down to the vacuum conditions of 2×10^{-4} mbar. Then the sample was stored at these conditions for 30 min allowing additional cleaning and gas removal from the sample's surface. Then, in the case of treatment at particular gas environment, the valve between chamber and pump line was closed and the gas was inserted inside the chamber. For all gases the same pressure at about 200 mbar was used. After gas purging, the sample was textured by laser radiation. Finally, before opening chamber, the treated sample was stored for 2 hours in the same gas environment. Immediately after extracting from chamber, the sample was tested to measure WCA. In the case of laser treatment in atmospheric air or only in vacuum the same ageing time was used. Alongside with influence of the gas environment, the variation of scanning speed and polarization caused the morphology and wettability variations.

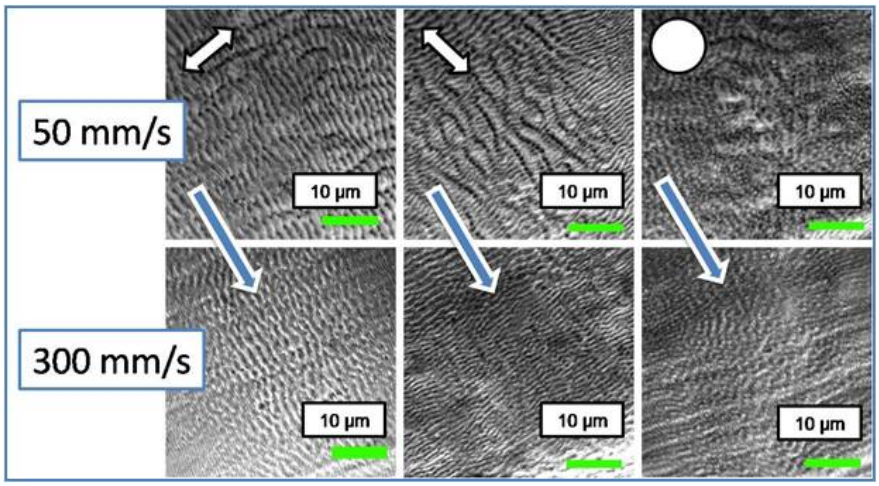

Figure 3. SEM images of the laser-textured samples prepared in ambient air. Blue arrows show the direction of scanning by laser beam. Direction of polarization is marked with white arrows in the case of linear polarization and with white circle in the case of circular polarization.

The morphology of the laser-textured surfaces prepared in ambient air is shown on Fig. 3. The direction of scanning is shown by blue arrows, and polarization direction is shown by white arrows. Changing scanning speed with saving single pulse fluence led to formation of the periodic submicron- and micron-sized ripples at low number of overlapped beams (Fig. 3, 300 mm/s) and microgrooves at intermediate number of overlapped beams (Fig. 3, 50 mm/s) and in principal can form the quasiperiodic arrays of microspikes at high number of pulses and linear polarization [19, 20]. In our case, at very low scanning speed, corresponding to optimal conditions for the microspikes formation, i.e. at high number of overlapped shots, the meshes started to deform due to accumulating heat and destruction of wires. Because of this we limited our experiments with 50 mm/s lowest speed.

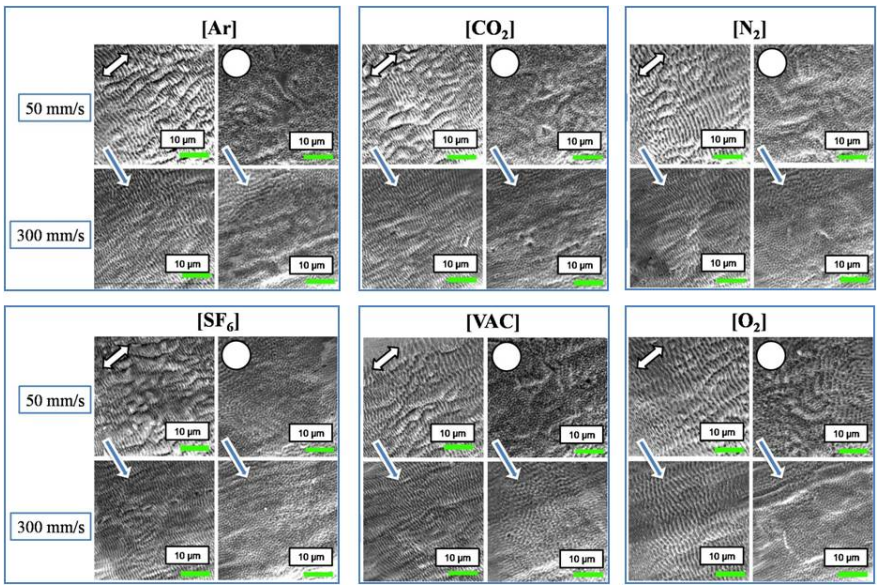

Figure 4. SEM images of the laser textured samples prepared in various gas environment and in the vacuum. With blue arrow pointed direction of the scanning by laser beam. Direction of polarization marked with white double side arrows in case of linear polarization and with white circle for circular one.

During these experiments, laser induced periodic surface structures (LIPSS) in the form of ripples with the period close to laser wavelength and with the direction perpendicular to laser polarization were formed (Fig. 3, 300 mm/s row, left and central panels). With increasing number of overlapped pulses (i.e. decreasing scanning speed) the microgrooves were directed mainly parallel to polarization direction and with period of a few laser wavelengths appear (Fig. 3, 50 mm/s row, left and central panels). In the case of circular polarization, the ripples were replaced with micropikes and with increasing number of pulses bigger structures in form hills can be observed (Fig. 3, last column).

In the case of different gas environment, the resulted SEM images of the textured surfaces are shown on Fig. 4. Same, as for Fig. 3, tendency was observed. In general, there was no big difference in textured surfaces for different gases and vacuum. The resulting morphology was very similar for different gases suggesting that any observed wettability changes had no relations with roughness variations. Note that, in case of SF_6, a suppression of the formation of the nano-textured microstructures due to chemical reactivity was reported [21]. We didn't observe such effect, probably due to lower laser fluence and smaller number of overlapped pulses compared with the experimental conditions of [21].

Vacuum ageing

In this subsection, we address the effect of low-pressure vacuum ageing on the wettability transformation of metal surfaces textured in air [22,23]. It was reported that the ageing of laser-treated samples in vacuum allows increasing the hydrophobic properties for much shorter (up to a few hours) period of time, compared with the time required for long-term air ageing. This behavior was attributed to presence of hydrocarbons in form of contaminations from either oil used for lubrication of moving parts of vacuum pumps. We address this problem since in our experiments the mesh samples were treated by laser radiation inside the chamber at vacuum conditions or in gas environment under pressure (200 mbar) still lower that atmospheric one and then stored for a period of 2 hours. The goal was to clarify and separate the possible side effect from vacuum system.

For these purposes four sets of samples were prepared in atmospheric air. After preparation first set was tested for WCA after keeping sample during one hour in air. This measurement is served as a reference for

three other sets. Second set of samples was stored in ambient air for 12 hours at the conditions described in the experimental section. Third and fourth sets of samples were placed in Chamber #1 and Chamber #2, respectively, for 12 hours of vacuum storage. After ageing for given period of time the WCA's of one air set and two vacuum sets of samples were measured.

The results of this experiment are shown on Fig. 5. Black solid line with solid squares shows the dependence of WCA on the scanning speed in the case of the set kept in air within 1 hour after texturing. As it was expected, after texturing in air the sample's wettability changed to hydrophilic ($\vartheta_w < 90^o$). WCA increased once the scanning speed increased from 50 to 300 mm/s. Second set aged in air for 12 hours (Fig. 5, red solid line with solid circles) still demonstrated the hydrophilic properties. WCA for the low scanning speeds remained almost unchanged, while for higher speeds (250-300 mm/s) it increased compare to the one tested 1 hour from laser treatment, while still remaining lower than WCA of untreated mesh surface ($\vartheta_w = 128^o$).

Meanwhile, the third and fourth sets of samples aged in vacuum inside the Chamber #1 and Chamber #2 showed the dramatic difference in WCA once we compared these two samples and air stored samples. For all samples stored in Chamber #2 (Fig. 5, blue solid line with solid triangles), WCA shifted to the super-hydrophobic region (Fig.5, hatched grey area corresponding to WCA>150°), while the samples stored in Chamber #1 (Fig. 5, green solid line with solid triangles), though showing the increased WCA, still demonstrated smaller value of this parameter compared with the untreated surface. Some increase of wettability in the latter case can be explained by dehydration of samples in vacuum. Brown horizontal line in the Fig. 5 shows WCA for untreated surface of the meshes. This angle was equal ˜128° and remained same under different gas phases and low vacuum ageing.

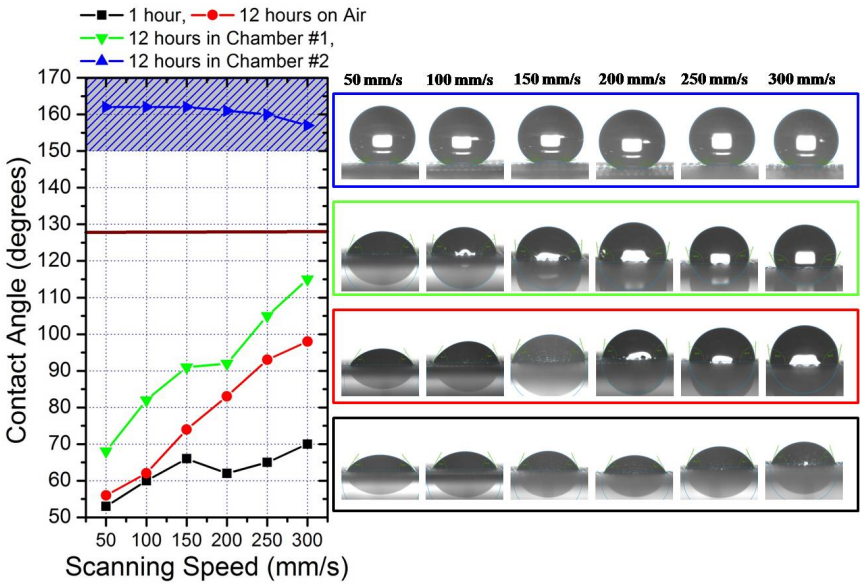

Figure 5. Results of the ageing of laser-textured meshes in air (red solid line with filled circles), in Chamber #1 (green solid line with filled triangles) and Chamber #2 (blue solid line with filled triangles). Reference samples measured after 1 hour after laser texturing are shown by black solid line with filled squares. On the right side the images of WCA recorded by Drop Shape Analyzer are shown.

Surface micro-nanostructures formed on the metal meshes by laser texturing is crucial and primary requirement for altering the wetting properties of the materials. WCA measurement of the freshly laser structured stainless steel meshes in ambient air conditions demonstrated hydrophilic behavior due to high generation of the metal oxides. The unsaturated cations-anions formed after laser ablation stabilize themselves by het-

erolytic dissociative adsorption of H_2O molecules from the atmosphere, giving birth to hydroxylated layer over metal-oxides layer [24]. The hydroxylated (-OH) layer has high affinity to adsorb water molecules through hydrogen bonding that explains the hydrophilic nature of freshly laser textured surfaces.

Surface chemistry was semi-quantitatively analyzed using EDS measurements. Figure 6 shows the variation of the weight percentage (wt%) of carbon (black bars) and oxygen (cyan bars) elements in the case of laser treated and untreated surfaces. A significant growth of O and decrease of C on the freshly prepared mesh microstructures is observed (R11 and R12 bars, Fig. 6). This effect related to the material removal by ablation process can lead to surface cleaning and on the other hand to the oxidation of the surface material with atmospheric oxygen. Also note that, with decreasing scanning speed (from 300 to 50 mm/s), the amount of oxygen increases due to the growing number of the overlapped laser pulses on the target surface (compare blue bars R11 and R12). After ageing in air and Chamber #1 for 12 hours (bars from R21 to R32) the relative content of C and O remain approximately the same, which explains the similar results for WCA in Fig. 5. In contrast, the ageing inside Chamber #2 (R41 and R42 bars in Fig. 6) led to the notable increase of carbon with regard to oxygen.

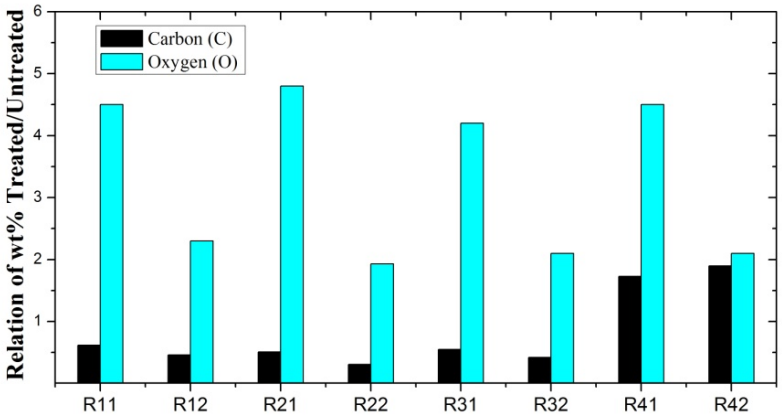

Figure 6. R11 and R12: EDS analysis of the relative weight variation of C (black bars) and O (cyan bars) in the case of laser-treated and untreated surfaces. Here R11 is a ratio of elements in the case of treated sample prepared in ambient air at 50 mm/s scan speed and stored for 1 hour in air after laser texturing. R12 is the same as R11, but at the scan speed 300 mm/s. R21 is the relation for sample prepared at 50 mm/s and stored for 12 hours in ambient air, R22 same as R21, but at 300 mm/s. R31 is the relation for sample prepared at 50 mm/s and stored for 12 hours in vacuum inside Chamber#1, R32 is the same as R31, but at 300 mm/s. R41 is the sample prepared at 50 mm/s and stored for 12 hours in vacuum inside Chamber#2, R42 is same as R41, but at 300 mm/s.

Thus, one can conclude that vacuum condition with hydrocarbons contamination can strongly change the surface chemistry of laser-treated samples. The short chained non-polar hydrocarbons replaced the –OH group formed immediately after laser ablation at an accelerated rate under vacuum storage. Thus, a faster transition in the wetting state from superhydrophilic to superhydrophobic state is observed after vacuum ageing in contaminated chamber. By this reason all SEM and EDS measurements were carried out for separately prepared samples. For further studies of different gas environment we used the Chamber #1.

Atmospheric air produced samples' ageing

Figure 7 shows the results of long-term ageing of samples produced in ambient air and later stored in air at normal atmospheric pressure. Here, wettability dependence on scanning speed, morphology produced by different polarizations (designated by horizontal polarization (HP), vertical polarization (VP) and circular polarization (CP)) and number of days are plotted. Again, the brown line depicts WCA for untreated surface (128°). 30 days ageing (blue solid lines) was enough for the most of samples to increase WCA above 140°. HP-, VP- and CP-treated samples irradiated using scanning speeds from 50 to 250 mm/s exceeded 145° and were close to the superhydrophobic limits, while some of them demonstrated WCA>150°. Whereas, improved water contact angle for the samples processed using lower scanning speeds (50 and 150 mm/s) was observed which can be attributed to the deeper and sharper surface morphology, since application of low scanning velocities results in rougher surface, with expressed ripples and additional structures and redeposition, while at high scanning speeds the surface remains less deformed. Rougher surface's absorbance probably becomes higher, which can attract the hydrocarbons presented in ambient air.

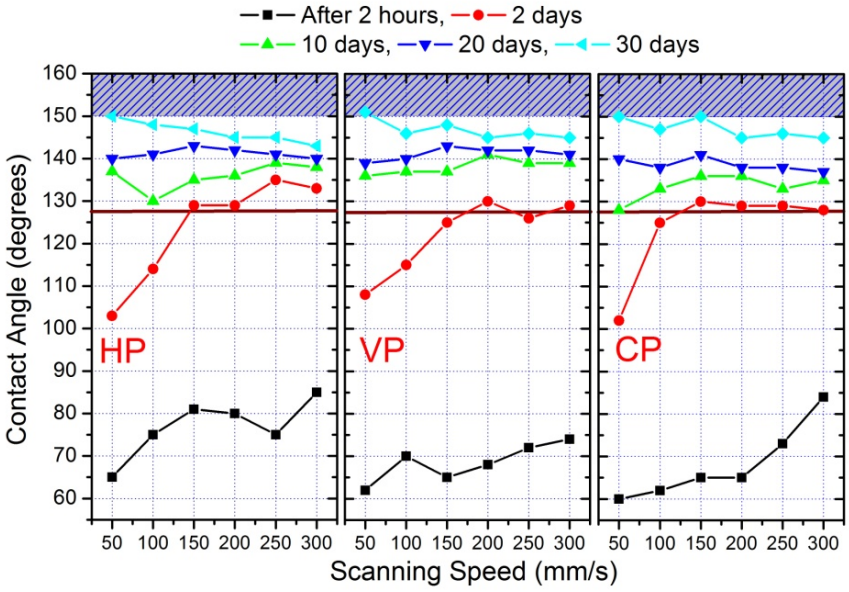

Figure 7. Evolution of WCA of the samples produced in the ambient air and aged up to 30 days in air. HP is the polarization direction of laser field perpendicular to direction of scanning, VP is the direction of laser field parallel to direction of scanning and CP is circularly polarized laser beam.

Strongly irradiated surface at initial periods of air ageing demonstrates hydrophilic properties, but for later times (>2 days) the pace of changing is increasing and outperforms initial WCA. Final result of ageing in Fig. 7 demonstrates no noticeable dependence on the morphology generated by applying different laser polarizations.

Figure 8 shows relation of the presence of the C (black bars) and O (cyan bars) for mesh samples after 30 days of ageing. For all samples we see the increase of the relative amount of carbon C on the textured surface. This amount lower than in case of samples stored inside Chamber #2 (Fig. 5), that can explain lower WCA in the case of air aged samples.

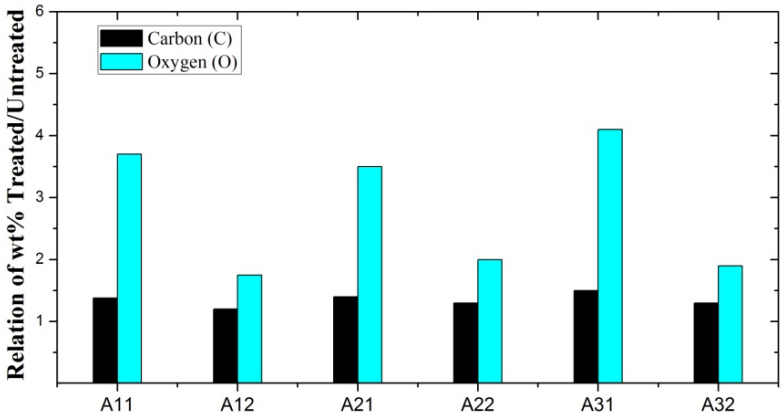

Figure 8. EDS analysis of the variations of weight percentage of C (black bars) and O (cyan bars) for laser-treated and untreated surfaces after 30 days ageing in atmospheric air. Here A11 is the relation of the treated/untreated sample prepared in ambient air at 50 mm/s scan speed, with HP polarization, A12 is the same as A11, but using the scan speed 300 mm/s. A21 is the relation for the sample prepared at 50 mm/s, with VP polarization, A22 is the same as A21 but using the scan speed 300 mm/s. A31 is the relation for the sample prepared using 50 mm/s scan speed, with CP polarization, A32 is the same as A31 but using the scan speed 300 mm/s.

Samples, prepared in gas and vacuum

Here we present the results of studies of the ageing of the samples prepared with the same laser parameters as were used in above studies but in presence of different gas media. These studies were performed inside the 'oil-less' Chamber #1 to exclude the possible side effects caused by combination with hydrocarbons. Our experiments with gases allow us to isolate and analyze the influence of three main components of atmospheric air (N_2, O_2 and CO_2) on the variations of wettability. This approach also excludes or at least dramatically decreases the influence of the water vapor inevitably presented in any atmospheric conditions.

The samples were prepared in the pure gases and stored in the same gas for 2 hours to achieve the relaxation after laser treatment, and then extracted from chamber and aged in ambient air for 30 days. The results of 30 days air ageing of the samples prepared in corresponding gaseous media are presented in Fig. 9. One can see the common property of all gases except oxygen: WCA's are mainly less than 140°, thus showing the reduced speed of transition to hydrophobic state. Only one set of samples prepared in O_2 environment demonstrated similar behavior as the air prepared samples. Probably, this observation emphasizes the role of oxides as the preferable substrate for facilitating the adsorption of hydrocarbon layer on the surface of laser-textured sample.

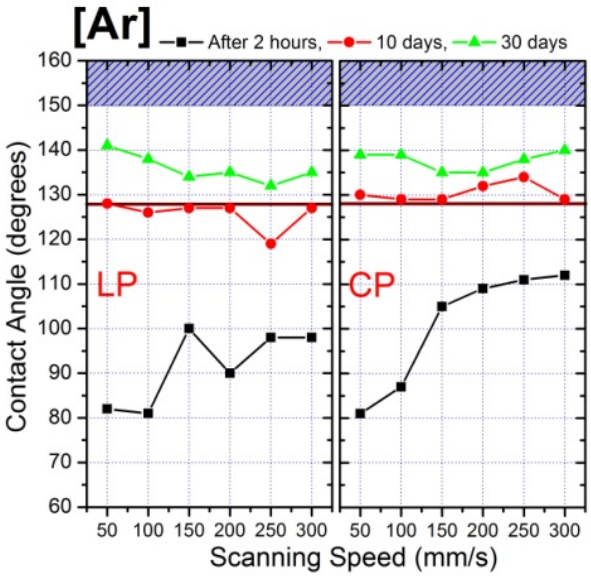

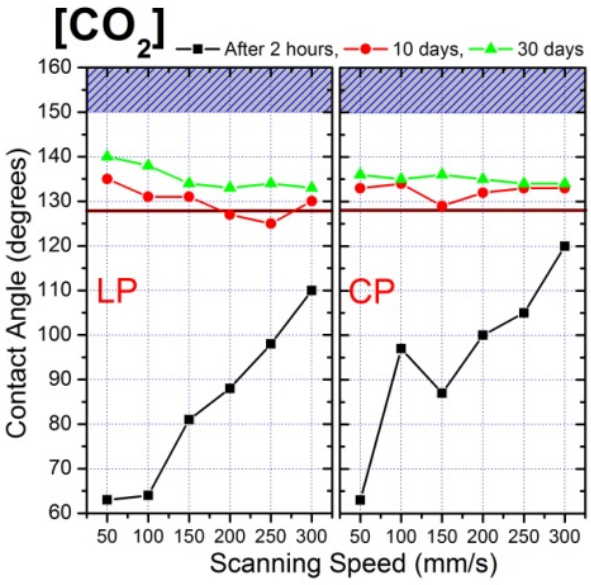

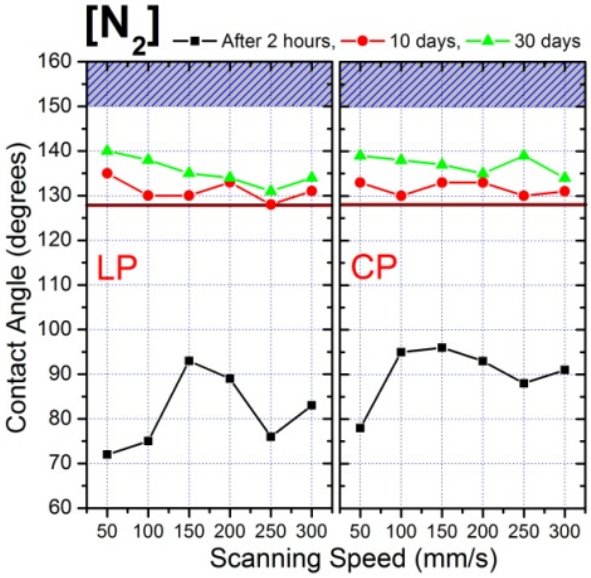

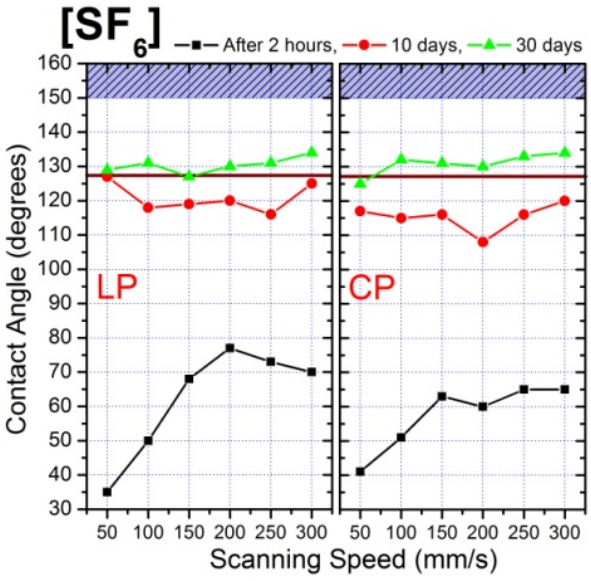

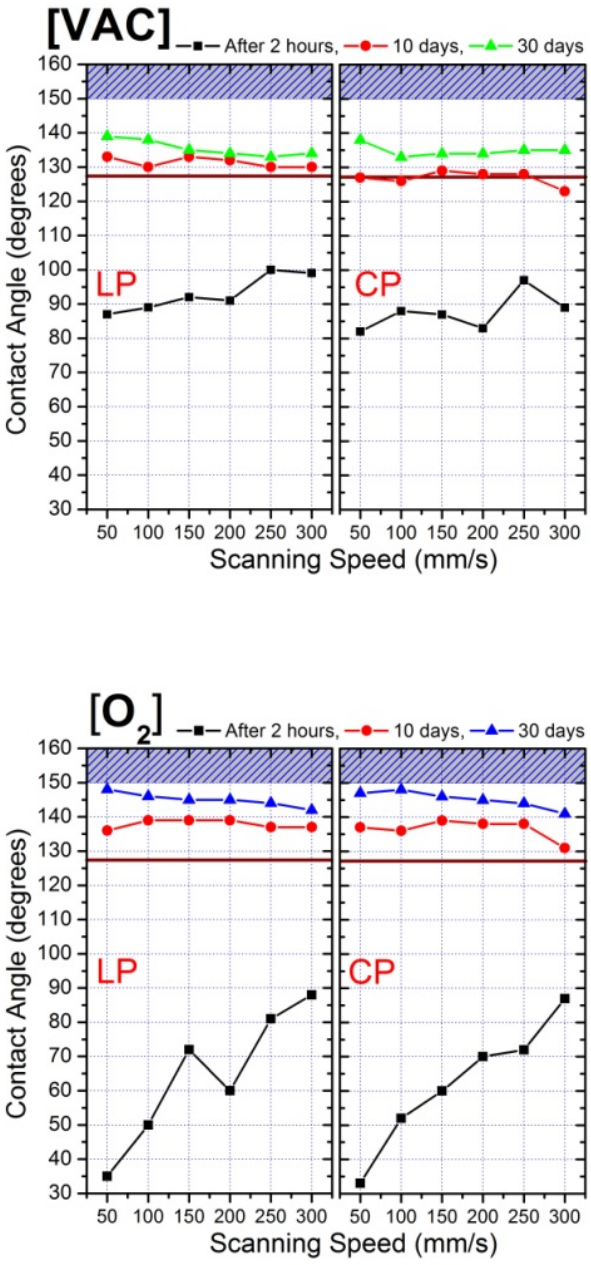

Figure 9. Evolution of WCA of the samples produced in the Ar, N_2, CO_2, SF_6, vacuum and O_2 and aged up to 30 days in ambient air. LP is the polarization direction of laser field perpendicular to the direction of scanning beam. CP is the circularly polarized laser beam.

The samples prepared in SF_6 showed slowest WCA transition speed. Also notice that surface of the samples prepared in SF_6 being tested in the defined spot for WCA, change the wetting properties after contact with water droplet. The repeated tests at the same place of these samples demonstrated higher WCA.

Figure 10 presents the summary of semi-quantitative analysis of variation of weight percentage relation for laser-treated samples in different gas media and untreated surfaces after 30 days of ageing in atmospheric

air. The marks below corresponding bars denote the used gases (from Ar to O_2, VAC means vacuum). HP and CP correspond to the polarization type, and the numerical values (1 and 2) correspond to the 50 mm/s and 300 mm/s scan speeds. In the case of O_2 (from O2 HP1 to O2 CP2 bars in Fig. 10, panel c), one can admit a pattern similar to Fig. 8, where stronger oxidation is accompanied with the increased presence of carbon, that can be associated with higher WCA.

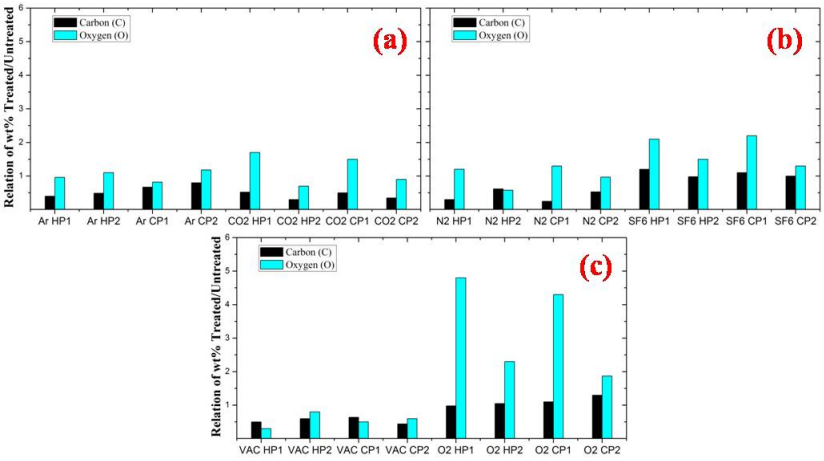

Figure 10. EDS analysis of the change of the weight percentage (wt%) relation between the samples treated by laser radiation in different gases and untreated surfaces for C (black bars) and O (cyan bars) elements after 30 days of ageing in atmospheric air. Subscripts of bars denote the gas type (Ar, CO_2, N_2, SF_6, O_2) and VAC corresponds to the vacuum conditions. HP and CP correspond to horizontal and circular polarizations, similar to Fig. 7. Numbers 1 and 2 indicate the scan speeds used (50 and 300 mm/s, respectively).

For SF_6 bars (from SF6 HP1 to O2 CP2 bars in Fig. 10, panel b) we also observed relatively high presence of the carbon. Meanwhile, only in this case among all gases we observed the relatively high presence of one of the component of SF_6 gas, fluorine F (up to 8 wt% in case of 50 mm/s scanned sample) such increasing of fraction of light elements (C, O, F) compare to main heavy Fe element leads to common increase of wt% for all light elements and this can explain relatively high presence of C not accompanied with increasing of WCA. The presence of F can lead to formation of the metal-fluoride compounds, which may explain the unstable behavior of the samples. For other gases (Ar, N_2, CO_2) (from Ar HP1 to CO2 CP2 bars in Fig. 10, panel a and bars N2 HP1 to N2 CP2 in Fig 10, panel b) and vacuum (bars VAC HP1 to VAC CP2 in Fig 10, panel c), the common features were the small additional oxidation and lesser presence of carbon, which is well correlates with lesser values of WCA measurements shown in Fig. 9. Also notice on the insignificant difference for results produced at linear (HP) and circular (CP) polarizations either in the case of WCA or EDS measurements.

Conclusions

Our studies have revealed the role of different gas environment at which stainless steel meshes were laser-textured for long-term air ageing. We also introduced the surface morphology difference by producing two types of structures (ripples and spikes) when the accumulated laser fluence was varied by changing the scanning speed. We did not observe a significant dependence of the low-scale LIPSS morphology, while observing a weak dependence on the scanning speed variations in the studied range of variations of this parameter. After 30 days of ageing the samples produced in atmospheric air and in pure O_2have demonstrated the transition towards large contact angles (WCA $> 145°$), while the samples prepared in Ar, CO_2, N_2, SF_6 and vacuum maintained their WCA below or at around 140°. EDS analysis have demonstrated the correlation of the amount of O and C with the observed hydrophobicity. Probably, gases, except O_2, reduce the final WCA after 30 days of aging, which was attributed to lesser oxidation preventing the formation of phobic

layer. For the stainless steel mesh, O_2 and hence oxidation play important role in providing optimal conditions for transformation to hydrophobic state.

Funding: These studies were supported by FRG AS1801 grant and the Common Research Facility at the American University of Sharjah.

References

1. Muller, F.; Kunz, C.; Graf, S. Bio-Inspired Functional Surfaces Based on Laser-Induced Periodic Surface Structures. Materials 2016, 9, 476

2. Nuutinen, T.; Silvennoinen, M.; Paivasaari, K.; Vahimaa, P. Control of Cultured Human Cells with Femtosecond Laser Ablated Patterns on Steel and Plastic Surfaces. Biomed. Microdevices 2013, 15, 279-288

3. Long, J.; Fan, P.; Gong, D.; Jiang, D.; Zhang, H.; Li, L.; Zhong, M. Superhydrophobic Surfaces Fabricated by Femtosecond Laser with Tunable Water Adhesion: From Lotus Leaf to Rose Petal. ACS Appl. Mater. Interfaces 2015, 7, 9858-9865

4. Skoulas, E.; Manousaki, A.; Fotakis, C.; Stratakis, E. Biomimetic Surface Structuring Using Cylindrical Vector Femtosecond Laser Beams. Sci. Rep. 2017, 7, 45114

5. K. Yin, D. Chu, X. Dong, C. Wang, J.-A. Duan, J. He, Femtosecond laser induced robust periodic nanoripple structured mesh for highly efficient oil–water separation, Nanoscale. 9 (2017) 14229–14235. https://doi.org/10.1039/C7NR04582D

6. Ali S. Alnaser, Sharjeel A. Khan, Vadim Lalyshev, Vyacheslav V. Kim, Mazhar Iqbal, Hamad Al Harmi, Ganjaboy S. Boltaev and Rashid A. Ganeev, Expedited Transition in the Wettability Response of Metal Meshes Structured by 50-kHz Femtosecond Pulses for Oil-Water Separation, Front. Chem. doi:10.3389/fchem.2020.00768

7. S.J. Park, M.K. Seo, Solid-liquid Interface, Interface Sci. Compos, Elsevier, Amsterdam, The Netherlands 2011, pp. 147–252, https://doi.org/10.1016/B978-0-12-375049-5.00003-7

8. F. Chen, D. Zhang, Q. Yang, X. Wang, B. Dai, X. Li, X. Hao, Y. Ding, J. Si, X. Hou, Anisotropic wetting onmicrostrips surface fabricated by femtosecond laser, Langmuir 27 (2011) 359–365, https://doi.org/10.1021/la103293j

9. A. Riveiro, T.Abalde, P.Pou, R.Soto, J.del Val, R.Comesaña, A.Badaoui, M.Boutinguiza, J.Pou, Influence of laser texturing on the wettability of PTFE Appl. Surf. Sc, 515 (2020) 145984, https://doi.org/10.1016/j.apsusc.2020.145984

10. J. Long, M. Zhong, H. Zhang, P. Fan, Superhydrophilicity to superhydrophobicity transition of picosecond laser microstructured aluminum in ambient air, J. Colloid Interface Sci. 441 (2015) 1–9 https://doi.org/10.1016/j.jcis.2014.11.015.

11. A.M. Kietzig, S.G. Hatzikiriakos, P. Englezos, Patterned superhydrophobic metallic surfaces, Langmuir 25 (2009) 4821–4827, https://doi.org/10.1021/la8037582

12. Y. Tian, L. Jiang,Wetting: intrinsically robust hydrophobicity, Nat.Mater. 12 (2013) 291–292, https://doi.org/10.1038/nmat3610

13. V.D. Ta, A. Dunn, T.J. Wasley, J. Li, R.W. Kay, J. Stringer, P.J. Smith, E. Esenturk, C. Connaughton, J.D. Shephard, Laser textured superhydrophobic surfaces and their applications for homogeneous spot deposition, Appl. Surf. Sci. 365 (2016) 153–159, https://doi.org/10.1016/j.apsusc.2016.01.019

14. J.T. Cardoso, A. Garcia-Girón, J.M. Romano, D. Huerta-Murillo, R. Jagdheesh, M. Walker, S.S. Dimov, J.L. Ocaña, Influence of ambient conditions on the evolution of wettability properties of an IR-, ns-laser textured aluminium alloy, RSC Adv. 7 (2017) 39617–39627, https://doi.org/10.1039/c7ra07421b

15. D.V. Ta, A. Dunn, T.J. Wasley, R.W. Kay, J. Stringer, P.J. Smith, C. Connaughton, J.D. Shephard, Nanosecond laser textured superhydrophobic metallic surfaces and their chemical sensing applications, Appl. Surf. Sci. 357 (2015) 248–254, https://doi.org/10.1016/j.apsusc.2015.09.027

16. Z. Yang, Y.L. Tian, C.J. Yang, F.J. Wang, X.P. Liu, Modification of wetting property of Inconel 718 surface by nanosecond laser texturing, Appl. Surf. Sci. 414 (2017) 313–324, https://doi.org/10.1016/j.apsusc.2017.04.050

17. P. Pou, J. del Val, A. Riveiro, R. Comesana, F. Arias-Gonzalez, F. Lusquinos, M. Bountinguiza, F. Quintero, J. Pou, Laser texturing of stainless steel under different processing atmospheres: from superhydrophilic to superhydrophobic surfaces, Appl. Surf. Sci. 475 (2019) 896–905, https://doi.org/10.1016/j.apsusc.2018.12.248.

18. M.M. Gentleman, J.A. Ruud, Role of hydroxyls in oxide wettability, Langmuir 26 (2010) 1408–1411, https://doi.org/10.1021/la903029c

19. Y.H.Han and S.L.Qu, Chem. Phys. Lett. 495, 241 (2010)

20. T. H. Her, R. J. Finlay, C.Wu, S. Deliwala, and E.Mazur, Appl. Phys. Lett. 73, 1673 (1998), A. J. Pedraza, J. D. Fowlkes, and Y. F. Guan, Appl. Phys. A 77, 277 (2003)

21. B.K. Nayak, M.C. Gupta1, K.W. Kolasinski, Formation of nano-textured conical microstructures in titanium metal surface by femtosecond laser irradiation, Appl. Phys. A 90, 399–402 (2008)

22. R. Jagdheesh, J.L. Ocana, Laser machined ultralow water adhesion surface by low pressure processing, Materials Letters 270 (2020) 127721

23. R. Jagdheesh, P. Hauschwitz, J.Mužík, J. Brajer, D. Rostohar ,P.Jiříček, J. Kopeček, T. Mocek, Non-fluorinated superhydrophobic Al7075 aerospace alloy by ps laser processing, Applied Surface Science 493 (2019) 287–293

24. A.S. Alnaser, S.A. Khan, R.A. Ganeev, E. Stratakis, Recent advances in femtosecond laser-induced surface structuring for oil–water separation, Appl. Sci. 9 (2019) 1554. https://doi.org/10.3390/app9081554.